Intrazeolite Complexation of Transition Metal Ions by Triazacyclononane-Type Ligands: Control of Cluster Nuclearity and Oxygen Binding in Confined Reaction Spaces

Dirk De Vos[†] and Thomas Bein*

Contribution from the Department of Chemistry, Purdue University, West Lafayette, Indiana 47907

Received August 19, 1996. Revised Manuscript Received July 3, 1997[⊗]

Abstract: 1,4,7-Triazacyclononane (L) and its methylated analog (L′) form complexes with zeolite-exchanged Mn^{2+}, Co^{2+}, or Cu^{2+}. Through comparison with diluted solutions of the complexes, the effect of the zeolite environment on the complex formation was evaluated. In the case of Mn^{2+}, the complexation was monitored by observing the zero-field splitting in the X- and Q-band ESR spectra of the Mn^{2+} ion. Adsorption of L into metal Y zeolites yields *bis* L complexes; the L′ *mono* complexes are formed. The latter complexes are not coordinated by the zeolite surface, as deduced from the spectral parameters of the $[Mn(L')]^{2+}$ and $[Cu(L')]^{2+}$ complexes. *Mono* $[Co(L')]^{2+}$ in the zeolite is a reversible dioxygen binder, a property not previously documented for these complexes in solution. Exposure of $[Mn(L)_2]^{2+}$ or $[Mn(L')]^{2+}$ containing Y zeolites to H_2O_2 results in intraporous formation of oxidized Mn dimers. The constrained zeolite environment seems to stabilize the oxidized dimers of Mn and L by preventing further cluster expansion.

Introduction

The introduction of metal complexes into zeolites has produced a growing number of heterogeneous hydrocarbon oxidation catalysts.[1] In many cases, the entrapment of the complex in the zeolite is crucial to promote the catalytic properties of the encapsulated complex.[2] Therefore a detailed understanding of the effect of the zeolite on the intraporous complexation is necessary. Major classes of ligands studied to date include Schiff bases, phthalocyanines, (poly)pyridines, and some amines. The catalytic potential of Mn complexes of cyclic triamine ligands has recently been demonstrated, both for complexes in solution and for the zeolite-immobilized counterparts.[3] Typical ligands are 1,4,7-triazacyclononane (L) and its substituted variants such as 1,4,7-trimethyl-1,4,7-triazacyclononane (L′). The inorganic chemistry of these compounds has been documented in detailed studies.[4] The most charac-

teristic property of *cis* binding tridentate ligands such as L and L′ is that in solution they easily form di- or polynuclear complexes.

This paper investigates the complexation of several transition metal ions with L and L′ in microporous zeolite environments. As zeolite surfaces are known to act as multidentate ligands for transition metal ions, the intrazeolite complexation is actually a competition between two chelands for one metal ion. The spatial constraints imposed by the dimensions of the zeolite cage or channels and by the surface curvature are expected to result in deviations from the known solution chemistry. In view of the relevance for oxidation catalysis, the focus is on the spectroscopy of Mn-L and Mn-L′ complexes in zeolites, before and after exposure to oxidants.[3d] ESR and UV−visible spectroscopy for Cu and Co systems are used to obtain a coherent picture of the metal−triamine−zeolite systems.

Experimental Section

Zeolites (Na-Y, ZSM-5, and Na-A) were obtained from PQ. The Si to Al ratio of the ZSM-5 zeolite was 10. The ZSM-5 zeolite was converted into its Na^+ form via neutralization with NH_3 and exchange with 1 M NaCl. Mn^{2+} exchange was performed in 2 mM $MnCl_2$ solutions at pH 6. Addition of about 3 g of wet Na^+ zeolite (corresponding to 2.5 g of dry zeolite) to 190 mL of the $MnCl_2$ solution resulted in a Mn loading of 0.85 wt %, or 1 Mn per 4 supercages in the case of zeolite Y. This was the standard metal concentration throughout the experiments. Zeolites were dehydrated under flowing N_2 by heating at 1 K per min up to 523 K and keeping the sample at that temperature for 12 h. Ligand adsorption was performed by mixing the zeolite with the dry ligand under inert atmosphere in a quartz tube. The ligand:metal ratio used was 2.2:1, except when indicated otherwise. After evacuation the mixture was heated for 2 h at 373 K, and subsequently for at least 6 h at 423 K in a closed reactor. In the case of the MnNa-ZSM-5 and MnNa-A samples, some condensation of the ligand in the upper, unheated part of the quartz tube indicated that the ligand had limited or no access to the zeolite's inner pore volume.

---

* Address correspondence to this author.
[†] Present address: Centre for Surface Science and Catalysis, Katholieke Universiteit Leuven, Kardinaal Mercierlaan 92, 3001 Heverlee, Belgium.
[⊗] Abstract published in *Advance ACS Abstracts,* September 1, 1997.
(1) For some reviews on this subject, see: (a) De Vos, D. E.; Buskens, P. L.; Vanoppen, D. L.; Knops-Gerrits, P. P.; Jacobs, P. A. In *Comprehensive Supramolecular Chemistry*; Pergamon: Oxford, 1996; Vol. 7, Chapter 22. (b) Bein, T. *Comprehensive Supramolecular Chemistry*; Pergamon: Oxford, 1996; Vol. 7, Chapter 20. (c) Balkus, K. J., Jr.; Gabrielov, A. G. In *Inclusion Chemistry with Zeolites, Nanoscale Materials by Design*; Herron, N., Corbin, D., Eds.; Kluwer: Boston, 1995; p 159.
(2) (a) Herron, N.; Stucky, G. D.; Tolman, C. A. *J. Chem. Soc., Chem. Commun.* **1986**, 1521. (b) Bowers, C.; Dutta, P. K. *J. Catal.* **1990**, *122*, 271. (c) Knops-Gerrits, P. P.; De Vos, D. E.; Thibault-Starzyk, F.; Jacobs, P. A. *Nature* **1994**, *369*, 543. (d) Balkus, K. J., Jr.; Eissa, M.; Levado, R. *J. Am. Chem. Soc.* **1995**, *117*, 10753.
(3) (a) Hage, R.; Iburg, J. E.; Kerschner, J.; Koek, J. H.; Lempers, E. L. M.; Martens, R. J.; Racherla, U. S.; Russell, S. W.; Swarthoff, T.; van Vliet, M. R. P.; Warnaar, J. B.; van der Wolf, L.; Krijnen, B. *Nature* **1994**, *367*, 637. (b) De Vos, D. E.; Bein, T. *J. Chem. Soc., Chem. Commun.* **1996**, *917*. (c) De Vos, D. E.; Bein, T. *J. Organomet. Chem.* **1996**, *195*, 520. (d) De Vos, D. E.; Meinershagen, J. M.; Bein, T. *Angew. Chem., Int. Ed. Engl.* **1996**, *35*, 2211.
(4) (a) Chaudhuri, P.; Wieghardt, K. *Prog. Inorg. Chem.* **1987**, *35*, 329. (b) Bhula, R.; Osvath, P.; Weatherburn, D. *Coord. Chem. Rev.* **1988**, *91*, 89.
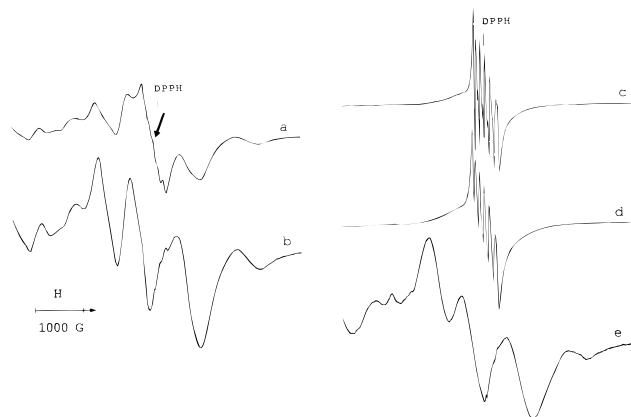
(5) (a) Searle, G. H.; Geue, R. J. *Aust. J. Chem.* **1984**, *37*, 959. (b) Wieghardt, K.; Chaudhuri, P.; Nuber, B.; Weiss, J. *Inorg. Chem.* **1982**, *21*, 3086.

Figure 1. X-band ESR spectra (9.4 GHz, 100 K) of (a) MnNaY + L, after 6 h at 423 K (L:Mn = 2.2:1), (b) MnNaY + L, after 12 h at 423 K (L:Mn = 4:1), (c) aqueous solution of $MnCl_2$, (d) aqueous solution of L and $MnCl_2$ in a 1:1 ratio, and (e) aqueous solution of L and $MnCl_2$ in a 4:1 ratio. In spectra c–e, 10 wt % of glycerol was added to permit instantaneous freezing. The arrow in spectrum a shows the weak remaining signal of lattice-coordinated Mn^{2+}. The Mn content of the Y zeolite is 0.85 wt %.

Table 1. ESR Parameters for Complexes of Mn^{2+} with the Macrocycles L or L′ in Aqueous Solution or in Zeolite Y

	a (G)	D (10^{-4} cm^{-1})
$[Mn(H_2O)_6]^{2+}$	96	100[a]
$[Mn(L)]^{2+}$ in aqueous solution, L:Mn = 1	90	≤200[b]
$[Mn(L)_2]^{2+}$ in aqueous solution, L:Mn ≥ 2	81	900[c]
$[Mn(L)_2]^{2+}$ in NaY	80	900[c]
$[Mn(L')]$ in aqueous solution	89	≤300[b]
$[Mn(L')]$ in NaY	87	550[c]

[a] Estimated from the relative intensities of the $\Delta m_S = \pm1$, $\Delta m_I = \pm1$ and the $\Delta m_S = \pm1$, $\Delta m_I = 0$ transitions. [b] Maximum values estimated from the width of the envelope structure under the central $m_S = +^1/_2 \leftrightarrow -^1/_2$ transition. [c] Calculated from the positions of the $m_S = \pm^1/_2 \leftrightarrow \pm^3/_2$ and $m_S = \pm^3/_2 \leftrightarrow \pm^5/_2$ transitions, or from the splitting of the central transition.

Oxidation of the Mn samples was performed by stirring 0.05 g of the Mn-L or Mn-L′ zeolite for 2 h in 1 mL of a 1 M solution of aqueous H_2O_2 or *tert*-butyl hydroperoxide in acetonitrile. When H_2O_2 was used as an oxidant, the system was cooled to 273 K to prevent excessive dismutation of the hydrogen peroxide. The solids were separated from the suspension by centrifugation, dried under a N_2 flow, and immediately introduced into the ESR cavity.

X-band ESR spectra (9.4 GHz) were recorded with a Bruker ESP-300 spectrometer. A rectangular TE_{104} cavity was used at temperatures between 7 and 300 K. For spectra of frozen solutions, a metal concentration of 1 mM was used, in methanol:water (90:10) or in water containing 10 wt % of glycerol. Q-band spectra (35 GHz) were recorded with a Varian spectrometer. Electronic spectra were recorded in diffuse reflectance mode with a Hitachi U-3501 spectrometer. ^{1}H-NMR spectra were recorded on a Varian 200 spectrometer. Ligands were from Aldrich (L′) or were synthesized following reported procedures (L);[5] their purity was checked with ^{1}H-NMR spectroscopy.

Results and Discussion

Complexation of Zeolitic Mn^{2+}. (a) Adsorption of L on MnNaY. Adsorption of L on a dehydrated MnNaY results in a gradual but drastic change of the X-band ESR spectrum. The narrow six-line signal of lattice-coordinated Mn^{2+} (a = 95 G) is replaced by a signal with discrete peaks, which extend between 0 and 6000 G. While after 6 h at 423 K some zeolite-chelated Mn^{2+} may still be observed, longer reaction times (12 h) or use of excess ligand (with a 4 to 1 L to Mn ratio) result in a total disappearance of the original Mn^{2+} signal (Figure 1, spectra a and b). This indicates that the displacement of the zeolite by the amine ligand can be driven essentially to completion.

The spectrum of this zeolite-confined Mn^{2+} compound was compared to those of frozen solutions of Mn^{2+} and L at different ratios. The *mono* and *bis* complexes $[Mn(L)]^{2+}$ and $[Mn(L)_2]^{2+}$ were prepared on the basis of the reported formation constants for the reaction between L and Mn^{2+} (Table 1).[6] In the absence of L, a = 96 G (A = 0.0090 cm^{-1}), and an average D value of 0.010 ± 0.002 cm^{-1} can be estimated from the intensity of the forbidden $\Delta m_S = \pm1$, $\Delta m_I = \pm1$ transitions relative to that of the $\Delta m_S = \pm1$, $\Delta m_I = \pm0$ lines (Figure 1c).[7] For $[Mn(L)]^{2+}$, the effect of the presence of ligand on the Mn spectrum is

surprisingly small. The spectrum is still dominated by the central $M_S = -^1/_2 \leftrightarrow +^1/_2$ transition around g = 2.00. In this transition the average a decreases to 90 G, which is consistent with a larger degree of covalency in the metal–ligand bonding.[8] In the sextet, allowed and forbidden lines can no longer easily be distinguished. This indicates that there is a larger zero-field splitting, which increases the intensity of the forbidden lines. This central transition is superimposed on an envelope, which arises from the broadened, non-central fine transitions (Figure 1d). From the width of this envelope, an upper limit for D of 0.020 cm^{-1} can be deduced.[9]

If the L:Mn ratio in the solution is increased to 2 or more, a spectrum is obtained which is highly similar to that of L containing MnNaY (Figure 1e). This similarity strongly indicates that, especially after a prolonged complexation, the intrazeolite species must be formulated as a *bis*-ligated [(Mn-(L)$_2$]$^{2+}$ complex. We have found no evidence for the formation of *mono* complexes in the zeolite. Simulation of the 9.4-GHz spectrum of the *bis* species is not straightforward, as the zero-field splittings are large in comparison with the Zeeman energy. Therefore measurements were also conducted at Q-band frequency (Figure 2). In the latter spectrum, the powder pattern of Mn^{2+} ($S = ^5/_2$), subject to an axial distortion of the crystal field, can now be recognized. Typically there are five major absorptions, which have been labeled **1** to **5** on the spectrum. These correspond to the θ = 90° maxima of the $\Delta M_S = \pm1$ transitions between the six $M_S = -^5/_2, -^3/_2, ..., +^5/_2$ states, with θ the angle between the local symmetry axis and the direction of the external magnetic field.[10] As can be seen in the spectrum, an axial distortion causes the five fine groups to be separated in first approximation by D, which is the axial zero-field splitting (ZFS) parameter. Hyperfine splitting by the Mn nucleus is only resolved for the central transition. For the noncentral transitions, the loss of hyperfine resolution is caused by strain on the ZFS parameters. This corresponds to the observation that resonance field positions for noncentral transitions are much more sensitive to parameter strain than for the central transition. Such behavior has previously been verified by studying Mn fine and hyperfine structure in crystals subject to mechanical stress.[11]

A second major consequence of $D \neq 0$ is the splitting of the central $M_S = -^1/_2 \leftrightarrow +^1/_2$ transition into a θ = 90° and a θ = 41.8° component (labeled as **3** and **3′** in Figure 2). These groups are shifted by $-2D^2/H_0$ and $+3.6$ D^2/H_0 respectively from H_0,

(6) Reported equilibrium constants for binding of a first and a second L on Mn^{2+} are $10^{5.8}$ and $10^{3.6}$, see: Squillante, M. R. Ph.D. Thesis, **1980**, Tufts University, MA, cited in ref 4a.

(7) Schaffer, J. S.; Farach, H. A.; Poole, C. P. *Phys. Rev. B* **1976**, *13*, 1869.

(8) Abragam, A.; Bleaney, B. *Electron Paramagnetic Resonance of Transition Ions*; Clarendon Press: Oxford, 1970; p 442.

(9) De Wijn, H. W.; Van Balderen, R. F. *J. Chem. Phys.* **1967**, *46*, 1381.

(10) Bleaney, B.; Ingram, D. J. E. *Proc. R. Soc. (London)* **1951**, *A205*, 336.

(11) (a) Feher, E. R. *Phys. Rev.* **1964**, *136*, A145. (b) Dowsing, R. D.; Ingram, D. J. E. *J. Magn. Reson.* **1969**, *1*, 517.
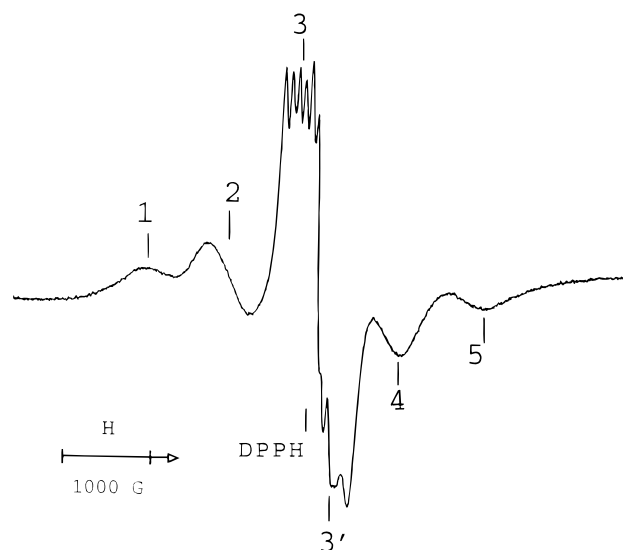
9462   *J. Am. Chem. Soc., Vol. 119, No. 40, 1997*

De Vos and Bein

Figure 2. Q-band band ESR spectrum (35 GHz, 100 K) of MnNaY + L, after 8 h at 423 K (L:Mn = 4:1). Symbols: **1** and **5**, $m_S = \pm^3/_2 \leftrightarrow \pm^5/_2$; **2** and **4**, $m_S = \pm^1/_2 \leftrightarrow \pm^3/_2$; **3**, $m_S = +^1/_2 \leftrightarrow -^1/_2$, $\theta = 90°$; **3′**, $m_S = +^1/_2 \leftrightarrow -^1/_2$, $\theta = 41.8°$. Vertical bars indicate calculated resonance positions for **1** through **5**.

where the resonance would occur in the absence of ZFS.[12] Due to the resolution of the hyperfine structure at 35 GHz, the center of the $M_S = -1/2 \leftrightarrow +1/2$, $\theta = 90°$ sextet can be determined with high precision, thus providing a second, independent check on the value of D. For calculation of the different resonance field positions, the Q-Pow simulation program was used,[13] and calculated field positions are included in Figure 2. For D, a value of 0.090 ± 0.005 cm^{-1} was obtained, while there is no evidence for E being different from zero. This parameter set, with a dominant axial zero-field splitting D, is consistent with the trigonal symmetry of the $[Mn(L)_2]^{2+}$ complex.[14]

(b) Adsorption of L on Smaller Pore Mn Zeolites. To assess whether this complexation reaction is an intraporous or an extraporous phenomenon, the diameter of the pores of the molecular sieve was varied. Thus Mn-exchanged Na-ZSM-5 and NaA were subjected to an identical dehydration and L adsorption procedure as MnNaY. While the ESR spectra of Mn^{2+} in zeolites of LTA (NaA) and FAU topology (NaX, NaY) have been studied in detail,[15,16] there is much less known about the spectroscopic signature of Mn^{2+} siting in MFI-type zeolites.[17] Some spectra are shown in Figure 3. Before dehydration of MnNaZSM-5, the intraporous Mn^{2+} is a regular aquo species, as demonstrated by the narrow sextet at $g = 2$ (spectrum not shown). After dehydration, a spectrum with broad wings is obtained (Figure 3a). This spectrum is reminiscent of those
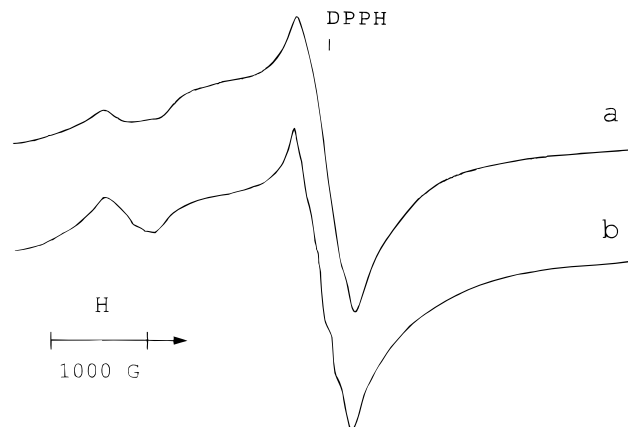
(12) Woltermann, G. M.; Wasson, J. R. *Inorg. Chem.* **1973**, *12*, 2366.

(13) Q-Pow was developed by M. Nilges at the University of Illinois at Urbana–Champaign.

(14) Comparison of our spectra with that of crystalline $[Mn(L)_2](ClO_4)_2$ is hampered by the lower resolution of the crystal spectrum, probably because of dipolar broadening: Gahan, L. R.; Grillo, V. A.; Hambley, T. W.; Hanson, G. R.; Hawkins, C. J.; Proudfoot, E. M.; Moubaraki, B.; Murray, K. S.; Wang, D. *Inorg. Chem.* **1996**, *35*, 1039. In the spectrum of the crystal, the hyperfine structure is not even resolved for the central fine transition; this hinders evaluation of D from the splitting of this transition. Even if one allows for loss of resolution, there are obvious differences at Q- and X-band between the spectra of zeolite-entrapped and crystalline $[Mn(L)_2]^{2+}$. It therefore seems likely that the trigonal symmetry of the intrazeolite and solution complexes is perturbed in the crystal, possibly because of hydrogen bonding with the perchlorate.

(15) Barry, T. I.; Lay, L. A. *J. Phys. Chem. Solids* **1968**, *29*, 1395.

(16) De Vos, D. E.; Weckhuysen, B. M.; Bein, T. *J. Am. Chem. Soc.* **1996**, *118*, 9615.

(17) Samuel, V.; Sivasanker, S. *Indian J. Chem.* **1990**, *29A*, 1086.

Figure 3. X-band ESR spectra (9.4 GHz, 100 K) of (a) MnNa-ZSM-5, dehydrated at 523 K, and (b) MnNa-ZSM-5 + L, after 8 h of heating at 423 K. The ZSM-5 zeolites contain 0.8 wt % of Mn.

of Mn^{2+} diluted in glasses[18] or in some solvents,[19] which have been interpreted as arising from a distributed population of Mn species with variable distortions, and hence variable D and E. This indicates that, in contrast to Mn in faujasites or A zeolites, the Mn in dry MnNa-ZSM-5 is either distributed over several sites, which have different coordination geometries, or characterized by a low local symmetry. When this dry MnNaZSM-5 is reacted with L, there are almost no observable changes in the ESR spectrum. This proves (i) that the relatively small ligand L is unable to penetrate the MFI structure and (ii) that the substantial spectral change in the case of MnNaY must be due to intraporous complexation. The contribution of Mn at the crystal surface to the observed chelation is clearly negligible, at least under these dehydrated conditions. The results for MnNaA lead to similar findings.

Adsorption of L′ on Mn Faujasites. As complexes of Mn^{2+} and L′ have not been characterized with ESR before, we prepared dilute Mn^{2+} solutions containing an excess of L′ for comparison of the spectra (Figure 4a,b). Literature reports indicate that for steric reasons formation of *bis* complexes from L′ is impossible;[4] thus even in an excess of L′, *mono* complexes are expected. Again it is observed that the presence of one triaza macrocycle around Mn^{2+} has relatively small effects on the fine structure. The hyperfine structure in the central transition changes upon complexation, with $a = 89$ G and stronger forbidden transitions (arrow). The envelope under the central transition suggests a ZFS not exceeding 0.030 cm^{-1}. Variation of the anion (Cl$^-$, SO$_4^{2-}$, or acetate) does not have a major influence on the spectra, indicating that the coordination sphere, probably of the NNNOOO type, is similar in all cases.[20] However, a difference in resolution is observed between spectra in methanol:water (90:10) and water–glycerol (90:10). In water–glycerol, several sextets of varying intensity can be distinguished toward the low-field side of the spectrum. These can be ascribed to the four $\Delta M_S = \pm 2$ transitions (Figure 4b). As the intensity of these transitions is proportional to $(D/g\beta H_0)^2$, their observation confirms that the complexation with L′ increases the zero-field splitting.

The X-band ESR spectrum of a MnNaY zeolite, after adsorption of L′, is shown in Figure 4c. It is clear at first glance

(18) Griscom, D. L.; Griscom, R. E. *J. Chem. Phys.* **1967**, *47*, 2711.

(19) Burlamacchi, L. *Gazz. Chim. Ital.* **1976**, *106*, 347.

(20) At higher concentrations of Mn(ClO$_4$)$_2$, and in the presence of acetate, acetate-bridged Mn^{II} dimers are formed: Wieghardt, K.; Bossek, U.; Bonvoisin, J.; Beauvillain, P.; Girerd, J.; Nuber, B.; Weiss, J.; Heinze, J. *Angew. Chem., Int. Ed. Engl.* **1986**, *25*, 1030. However, the six-line hyperfine structure of Figure 4a proves the mononuclear state of the complex under the conditions used in this study.
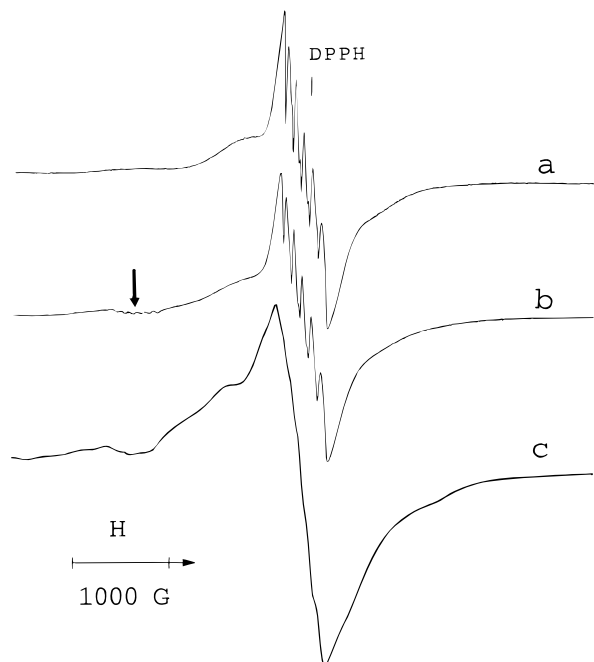
Figure 4. X-band ESR spectra (9.4 GHz, 100 K) of (a) a methanolic solution of $MnCl_2$ and L′, in a 1:2 ratio, (b) an aqueous solution of $MnCl_2$ and L′, in a 1:2 ratio, and (c) MnNaY + L′, after 8 h at 423 K (Mn:L′ = 1:2.2). In spectrum b, 10 wt % of glycerol was added to permit instantaneous freezing. The arrow in spectrum b indicates the sextet of one of the forbidden $\Delta m_S = \pm 2$ transitions.

that the zero-field splitting is considerably larger for the zeolite-entrapped complex than for the solution species. Instead of the envelope structure, several shoulders can now be recognized in the spectrum, upfield and downfield from the central transitions. From these D is estimated at 0.055 ± 0.005 cm^{-1}, while the plausible contribution of E cannot easily be quantified. In the Q-band spectrum shoulders can be discerned at positions which are consistent with this D value. The larger zero-field splitting in the zeolite is indicative of a more pronounced axial deviation from spherical symmetry. In solution and in the zeolite, Mn is expected to be surrounded by three N atoms of the L′ ligand. While in solution three solvent molecules complete the coordination sphere, in the dry zeolite only the dehydrated zeolite surface itself is available as a supplementary ligand. The more pronounced axial distortion of the Mn coordination sphere shows that Mn is only very weakly bound to the surface, if the zeolite is a ligand at all. This weak coordination can be ascribed to the spatial interaction between the L′ ligand in the [Mn(L′)]$^{2+}$ complex and the concave zeolite surface. An analogous steric effect is at the basis of the inability to bind a second L′ ligand on a [Mn(L′)]$^{2+}$ complex.[4] Because of the larger dimensions of the L′ ligand in comparison with the L molecule, adsorption of L′ on smaller pore zeolites was not attempted.

Exposure of L or L′ Containing Mn Zeolites to Peroxides. The NaY zeolites, containing [Mn(L′)]$^{2+}$ or [Mn(L)$_2$]$^{2+}$ were exposed to tBuOOH or H_2O_2. With tBuOOH, the typical signals of chelated Mn^{2+} disappear, and only a weak signal of some residual, probably zeolite-coordinated Mn^{2+}, remains. This indicates that the major part of the N-ligated Mn has been oxidized to ESR-silent Mn^{3+}. With H_2O_2, some residual Mn^{2+} may be observed, but the spectrum is dominated by the 16-line signal of a dimeric Mn^{3+}−Mn^{4+} complex (Figure 5). In the case of the L loaded zeolite, this implies that one of the two ligands is dissociated from Mn, which can be expected based on the reported lability of *bis* L complexes of trivalent Mn.[21]
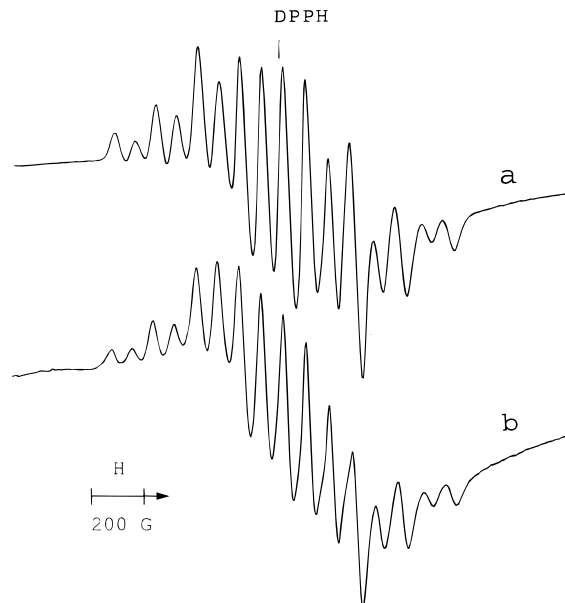

Figure 5. X-band ESR spectra (9.4 GHz, 100 K) of ligand containing MnNaY zeolites, after 2 h of exposure to H_2O_2 in CH$_3$CN. Ligands are (a) L and (b) L′.

Formation of clusters is a well-studied phenomenon in the interaction of Mn−triazacyclononane-type complexes with oxidants.[22] Although most available data were obtained via precipitation of pure complexes from complicated reaction mixtures, some firm conclusions have been drawn concerning the stability of the complexes with varying nuclearity. Under oxidative conditions, dimers are formed with Mn and L′. On the other hand, mixtures of L and Mn usually yield insoluble tetranuclear clusters, or other, thermodynamically more stable species such as MnO$_2$.[23] Only when bridging anions such as acetate are present in the medium is the formation of appreciable amounts of dinuclear complexes possible.[24,25] Other anions (*e.g.*, sulfate) hardly influence the aggregation state, or even cause disaggregation of clusters to occur (*e.g.*, Cl$^-$). If the observation of a 16-line ESR signal is considered to be an indication for the occurrence of dinuclear complexes in general, then the observation of the dinuclear Mn-L species in the zeolite sample, where no bridging acetate is present, is surprising. In a series of control experiments with solutions, using L, various Mn sources, and solvents, we have been unable to observe dinuclear oxidized Mn species, except when Mn acetate was used as the Mn source. This suggests that the steric confinement of the Mn complexes to the zeolite cage system kinetically stabilizes the dinuclear state. This hypothesis is confirmed by preliminary molecular modeling of the potential spatial interaction between the FAU lattice and the complex (manual docking in the cage).[3d] The further expansion toward the thermodynamically more stable tetranuclear state seems to be hindered because of the confinement of the dinuclear complexes to the restricted zeolite pore space. Similar effects of zeolite pore size on nuclearity have been studied extensively for Co−oxygen complexes in dehydrated zeolites. In the latter case a mononuclear Co^{III}L(O$_2^-$) (L = amine or Schiff base ligand) is

(21) Wieghardt, K.; Schmidt, W.; Herrmann; W.; Küppers, H. J. *Inorg. Chem.* **1983**, *22*, 2953.

(22) Wieghardt, K. *Angew. Chem., Int. Ed. Engl.* **1989**, *28*, 1153.

(23) Wieghardt, K.; Bossek, U.; Gebert, W. *Angew. Chem., Int. Ed. Engl.* **1983**, *22*, 328.

(24) Wieghardt, K.; Bossek, U.; Nuber, B.; Weiss, J.; Bonvoisin, J.; Corbella, M.; Vitols, S. E.; Girerd, J. J. *J. Am. Chem. Soc.* **1988**, *110*, 7398.

(25) Wieghardt, K.; Bossek, U.; Nuber, B.; Weiss, J.; Gehring, S.; Haase, W. *J. Chem. Soc., Chem. Commun.* **1988**, 1145.
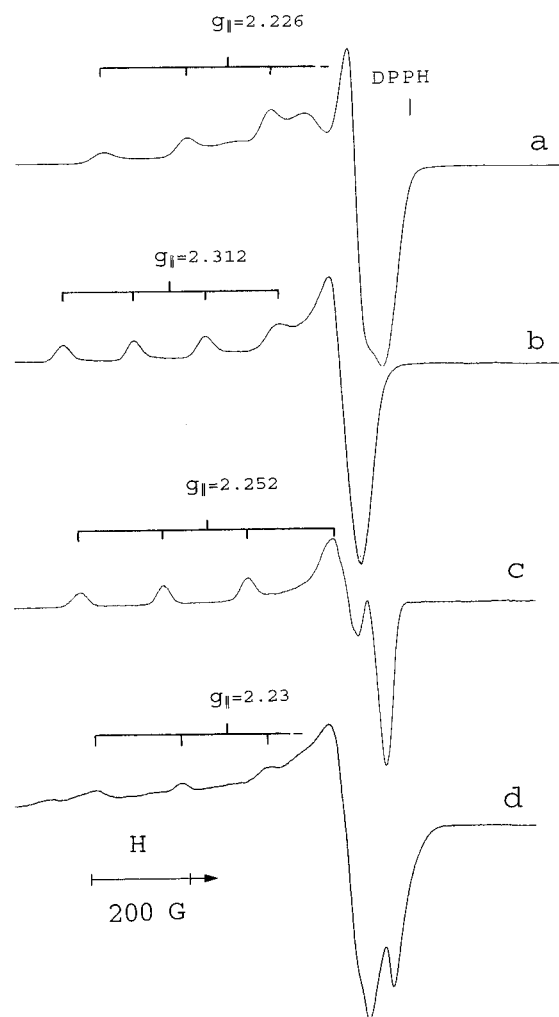
Figure 6. X-band ESR spectra (9.4 GHz, 100 K) of (a) CuNaY + L, after 8 h of heating at 423 K, (b) an aqueous solution of CuCl$_2$ and L′, in a 1:1 ratio, (c) an aqueous solution of CuCl$_2$ and L′, in a 1:2 ratio, (d) CuNaY + L′, after 8 h of heating at 423 K.

Table 2. ESR Parameters for Complexes of Cu^{2+} with the Macrocycles L or L′ in Aqueous Solution, in Crystals or in Zeolite NaY

	$g_{\parallel}$	$|A_{\parallel}|^a$	$g_{\perp}$	ref
CuNaY, dehydrated	2.39	140	2.06	32
	2.32	145	2.055	this work
CuNaY + L	2.226	170	2.05	this work
[Cu(L)Br$_2$]	2.278	158	2.050	27
[Cu(L)$_2$][Cu(CN)$_3$]	2.229	177	2.055	28
CuNaY + L′	2.230	170	2.05	this work
Cu^{2+} + L′ (1:1)^b	2.312	156	2.070	this work
Cu^{2+} + L′ (1:5)^b	2.252	177	2.057	this work

^{a} 10^{-4} cm^{-1}. ^{b} Measured in methanol:water (90:10). Identical results from copper chloride and sulfate.

stabilized and formation of dinuclear peroxo or superoxo complexes is retarded.[26]

Reactions of L and L′ in CuNaY. ESR spectra of dehydrated CuNaY zeolites, exposed to L or L′, are shown in Figure 6, and parameters, calculated by simulation with the Q-Pow program, are assembled in Table 2. In the case of L, *mono* and *bis* complexes can be easily distinguished.[27,28] The parameters for the zeolite sample leave no doubt that the main

product of the ligand adsorption is the [Cu(L)$_2$]$^{2+}$ complex. The situation is more complicated for the L′ adsorption. Reported g values for Cu^{2+} complexes of this ligand were mostly determined for polycrystalline, dimeric Cu complexes, for which no hyperfine structure is resolved.[29] Moreover, considerable exchange coupling occurs for such crystals, resulting in the g values drawing together. To obtain precise g values for mononuclear [Cu(L′)]$^{2+}$ chelates, we prepared dilute solutions of different Cu salts and L′ in several solvents. In all cases $g_{\parallel} > g_{\perp}$; hence it can be assumed that the unpaired electron is located in the d$_{x^2-y^2}$ orbital, as is the case for the frequently observed tetragonal Cu^{2+} complexes. Moreover the ratio ($g_{\parallel} - 2/g_{\perp} - 2$) exceeds 4, implying that the observed g values are those of the individual Cu centers; effects of exchange coupling are negligible.[30] In the absence of bridging anions (*e.g.* acetate), an increase of the L′:Cu^{2+} ratio, from 0 over 1 to over 2 produces two distinct Cu species, with $g_{\parallel} = 2.312$ and $g_{\parallel} = 2.252$, respectively (Figure 6, spectra b and c). As the formation of *bis* L′ complexes is impossible for steric reasons,[4] both species must be *mono* L′ complexes. One of these is undoubtedly the mononuclear [Cu(L′)]$^{2+}$ species, in which the coordination sphere is completed by solvent molecules. For the other complex, one might propose various tentative structures, *e.g.*, with a monoprotonated, partially chelating ligand. Similar structures with partially coordinating azacyclononanes have been described in the literature.[31] Irrespective of the precise assignment of the two solution species, the lower limit for their $g_{\parallel}$ value is 2.25.

The ESR spectrum of L′-containing CuNaY clearly is a superposition of several species, which are different from those observed for dehydrated CuNaY.[32] However, one species with $g_{\parallel} = 2.230$ dominates the spectrum. In view of the small $g_{\parallel}$ value, this complex must be one of Cu^{2+} and L′. The $g_{\parallel}$ for this intrazeolite [Cu(L′)]$^{2+}$ is even smaller than for similar species in solution, indicating that the lack of solvation of the complex by the zeolite surface increases the splitting of the energy levels, as was already observed for the intrazeolite *mono* [Mn(L′)]$^{2+}$ complex.

CoNaY. L and L′ react readily with a Co^{2+}-exchanged, dehydrated zeolite Y. This is easily observed by comparison of the reflectance spectra before and after ligand adsorption. Before the ligand adsorption, the zeolite is intensely blue, with triplets of bands in both the visible and NIR region, ascribed to Co^{2+} in a tetrahedral environment. The intensity of these bands decreases even when the Co^{2+} zeolite is mixed with the ligands at room temperature, and new bands are observed. However, there is substantial overlap between the new bands and those of residual lattice-coordinated Co^{2+}. As the latter tetrahedral species have high extinction coefficients (ϵ values typically amount to 100), it proved difficult to use the electronic spectra for assignment of Co^{2+} species. Only a band at 460 nm (21 700 cm^{-1}) in the spectrum of a heated CoY-L mixture could be attributed with certainty to the most intense transition ($\epsilon = 5.9$) of the [Co(L)$_2$]$^{2+}$ complex.[33] ESR does not give direct information on the complexation, as the complexes of Co with L and L′ are high spin. However, exposure of the ligand-containing zeolites to dry O$_2$ resulted in an intense signal for

(26) (a) Howe, R. F.; Lunsford, J. H. *J. Am. Chem. Soc.* **1975**, *97*, 5156. (b) De Vos, D. E.; Thibault-Starzyk, F.; Jacobs, P. A. *Angew. Chem., Int. Ed. Engl.* **1994**, *33*, 431. See also ref 1.

(27) Bereman, R. D.; Churchill, M. R.; Schraber, P. M.; Winkler, M. E. *Inorg. Chem.* **1979**, *18*, 3122.

(28) Chaudhuri, P.; Oder, K.; Wieghardt, K.; Weiss, J.; Reedijk, J.; Hinrichs, W.; Wood, J.; Ozarowski, A.; Stratemaier, H.; Reinen, D. *Inorg. Chem.* **1986**, *25*, 2951.

(29) Ozarowski, A.; Reinen, D. *Inorg. Chem.* **1986**, *25*, 1704. Chaudhuri, P.; Oder, K. *J. Chem. Soc., Dalton Trans.* **1990**, 1597.

(30) Procter, I. M.; Hathaway, B. J.; Nicholls, P. *J. Chem. Soc. (A)* **1968**, 1678.

(31) Reinen, D.; Ozarowski, A.; Jakob, B.; Pebler, J.; Stratemeier, H.; Wieghardt, K.; Tolksdorf, I. *Inorg. Chem.* **1987**, *26*, 4010.

(32) Herman, R. G.; Flentge, D. R. *J. Phys. Chem.* **1978**, *82*, 720.

(33) Küppers, H. J.; Neves, A.; Pomp, C.; Ventur, D.; Wieghardt, K.; Nuber, B.; Weiss, J. *Inorg. Chem.* **1986**, *25*, 2400.

Figure 7. X-band ESR spectrum (9.4 GHz, 100 K) of a dry CoNaY zeolite with adsorbed L′, after exposure to 100 Torr of dry oxygen.

the L′ containing CoNaY, while the L-CoNaY zeolite displayed no measurable ESR activity (Figure 7). On the basis of its reversible formation in oxygen exposure−evacuation cycles, the signal in the L′ zeolite was assigned to a $[Co^{III}(L')(O_2^-)]^{2+}$ adduct. This was confirmed by the g and A values from the simulation: $g_{\parallel} = 2.093$, $g_{\perp} = 2.00-2.01$, $a_{\parallel} = 16$ G, and $a_{\perp} = 10$ G.[34] All these observations are consistent with the formation of $[Co(L)_2]^{2+}$ and $[Co(L')]^{2+}$, respectively. The coordinatively saturated $[Co(L)_2]^{2+}$ cannot bind O_2. On the other hand, intrazeolite $[Co(L')]^{2+}$ complexes have a half-empty coordination sphere, as the zeolite cannot coordinate to the $[Co(L')]^{2+}$ complex. Consequently oxygen binding on these complexes is facile.

Conclusion

An overview of the spectroscopically observed complexations and complex transformations is presented in Scheme 1. Triazacyclononane readily enters 12-membered-ring zeolites such as NaY, and formation of *bis* triazacyclononane complexes could be demonstrated for intrazeolite Mn^{2+}, Co^{2+}, and Cu^{2+}. In the case of Mn^{2+}, the zero-field splitting parameters were used for the first time to follow such an intrazeolite chelation. Analysis of the spectral parameters for trimethyltriazacyclononane (L′) containing zeolites proves that the deviation of the $[M(L')]^{2+}$ complex from spherical symmetry is larger in the zeolite than for the same complex in solution. This implies that the zeolite is not bound to or is hardly capable of binding to the metal in a $[M(L')]^{2+}$ complex. As a result, the coordination sphere is almost half empty, and binding of molecules such as O_2 to the empty coordination sites could be demonstrated in the case of the Co^{2+} zeolite. The situation shows some similarities to what has been observed with tetradentate cyclic amines such as cyclam (1,4,8,11-tetraazacyclotetradecane) in zeolite Y.[35]

In the dehydrated zeolite, the $[Co^{III}(L')(O_2)]^{2+}$ superoxo

(34) Smith, T. D.; Pilbrow, J. R. *Coord. Chem. Rev.* **1981**, *39*, 295.

Scheme 1

complex is much more stable than in solution, where aggregation into dimers occurs. However, it seems that the zeolite can also exert an effect on the nuclearity of complexes in the hydrated state. Thus we observed a dinuclear Mn-L species under aqueous oxidative conditions, where in solution the formation of a more stable tetranuclear complex is preferred. This suggests that the spatial confinement of the dimer inside the zeolite pores can prevent cluster growth. Comparable phenomena have been observed in the formation of CdSe or GaP nanoclusters in zeolite voids.[36]

(35) In the specific case of intrazeolite cyclam complexes, the zeolite surface cannot function as a monodentate ligand for these bulky complexes. This is reflected not only in the spectral parameters, but also in a tendency to form *cis* instead of *trans* tetradentate chelates: De Vos, D. E.; Vanoppen, D. L.; Li, X. Y.; Bruynseraede, Y.; Knops-Gerrits, P. P.; Libbrecht, S.; Jacobs, P. A. *Chem. Eur. J.* **1995**, *1*, 144.

(36) (a) Moller, K.; Eddy, M. M.; Stucky, G. D.; Herron, N.; Bein, T. *J. Am. Chem. Soc.* **1989**, *111*, 2564. (b) McDougall, J. E.; Eckert, H.; Stucky, G. D.; Herron, N.; Wang, Y.; Moller, K.; Bein, T.; Cox, D. *J. Am. Chem. Soc.* **1989**, *111*, 8006.